

Autologous Micro-Fragmented Adipose Tissue as Stem Cell-Based Natural Scaffold for Cartilage Defect Repair

Cell Transplantation
2019, Vol. 28(12) 1709–1720
© The Author(s) 2019
Article reuse guidelines:
sagepub.com/journals-permissions
DOI: 10.1177/0963689719880527
journals.sagepub.com/home/ctt


Tengjing Xu¹, Xinning Yu^{1,2}, Quanming Yang¹, Xiaonan Liu¹,
Jinghua Fang^{1,2}, and Xuesong Dai^{1,2} 

Abstract

Osteoarthritis (OA) poses a tough challenge worldwide. Adipose-derived stem cells (ASCs) have been proved to play a promising role in cartilage repair. However, enzymatic digestion, ex vivo culture and expansion, with significant senescence and decline in multipotency, limit their application. The present study was designed to obtain micro-fragmented adipose tissue (MFAT) through gentle mechanical force and determine the effect of this stem cell-based natural scaffold on repair of full-thickness cartilage defects. In this study, ASCs sprouted from MFAT were characterized by multi-differentiation induction and flow cytometry. Scratch and transwell migration assays were operated to determine whether MFAT could promote migration of chondrocytes in vitro. In a rat model, cartilage defects were created on the femoral groove and treated with intra-articular injection of MFAT or PBS for 6 weeks and 12 weeks ($n = 12$). At the time points, the degree of cartilage repair was evaluated by histological staining, immunohistochemistry and scoring, respectively. Two unoperated age-matched animals served as native controls. ASCs derived from MFAT possessed properties to differentiate into adipocytes, osteocytes and chondrocytes, with expression of mesenchymal stem cell markers (CD29, 44, 90) and no expression of hematopoietic markers (CD31, 34, 45). In addition, MFAT could significantly promote migration of chondrocytes. MFAT-treated defects showed improved macroscopic appearance and histological evaluation compared with PBS-treated defects at both time points. After 12 weeks of treatment, MFAT-treated defects displayed regular surface, high amount of hyaline cartilage, intact subchondral bone reconstruction and corresponding formation of type I, II, and VI collagen, which resembled the normal cartilage. This study demonstrates the efficacy of MFAT on cartilage repair in an animal model for the first time, and the utility of MFAT as a ready-to-use therapeutic alternative to traditional stem cell therapy.

Keywords

micro-fragmented adipose tissue, stem cell, cartilage defect, repair

Introduction

Articular cartilage damage is one of the most central factors involved in the development of osteoarthritis, the most prevalent joint disease^{1,2}. Because of the lack of blood vessels, the injured cartilage cannot spontaneously regenerate without therapy^{3,4}. Unoperated strategies such as intra-articular injection of hyaluronic acid sodium, platelet-rich plasma, and concentrated cytokines are considered beneficial treatments for the early lesions^{5–8}. Subchondral microfracture and transplantation of autologous chondrocytes or cartilage combined with tissue engineering are traditional surgical treatments^{9–12}. However, none of these approaches is entirely satisfactory because of uncertain and inconsistent results^{13,14}. There is an urgent need to discover a better remedy to restore the structure and function of damaged cartilage.

¹ Department of Orthopaedic Surgery, The Second Affiliated Hospital, Zhejiang University School of Medicine, Hangzhou, China

² Department of Orthopaedic Surgery, Hangzhou Mingzhou Hospital (International Medical Center, Second Affiliated Hospital, Zhejiang University School of Medicine), Hangzhou, China

Submitted: July 23, 2019. Revised: August 26, 2019. Accepted: September 10, 2019.

Corresponding Author:

Xuesong Dai, The Second Affiliated Hospital, Zhejiang University School of Medicine, Shangcheng District, Jiefang Road 88#, Hangzhou city, Zhejiang Province 310009, China.

Email: daixshz@zju.edu.cn



In recent years, increasing attention to mesenchymal stem cells (MSCs) has led to new and effective therapies for cartilage regenerative medicine¹⁵. These multipotent cells can be harvested from various tissues, such as adipose tissue, bone marrow, periosteum, and synovium^{16–19}. Owing to their abundant source and easy access, adipose-derived stem cells (ASCs) have become the principal source of MSCs, with multidirectional differentiation properties into adipocytes, osteoblasts, chondrocytes, and other lineages, which have been investigated by experimental studies *in vitro* or *in vivo*^{20–22}. ASCs are routinely harvested by the enzymatic method and then expanded for several generations to sufficient quantity, with significant aging and a decline in multipotency as well as the destruction of the vascular matrix²³. Meanwhile, we find that the traditional enzymatic method to acquire ASCs may destroy surface structures which are important to cell viability and differentiation ability. Moreover, it takes a lot of time to expand into the desired amount *ex vivo*, leading to senescence. The heterologous enzymes and fetal bovine serum (FBS) used in the digestion and culture process have complex regulatory concerns related to good manufacturing practice (GMP) guidelines^{24–26}.

With the aim of avoiding these problems, we attempted to process adipose tissues with gentle mechanical force using a neoteric and completely closed device, Lipogems[®], where the fat is washed, emulsified, and micro-fragmented to remove blood and oil residues^{27,28}. The system reduces the adipose cluster dimensions, provides ready-to-use micro-fragmented adipose tissue (MFAT) in a short time without cell expansion, enzymatic treatment or other major manipulations, and maintains an intact stromal vascular niche, which is regarded as a reservoir of a heterogeneous cellular population including pericytes, the origin of ASCs²⁹. The purpose of our study was to determine whether MFAT could promote the repair of damaged cartilage with the key elements including natural scaffold (the adipose tissue structure), cells (ASCs), and growth factors (secreted cytokines and chemokines) to support the regenerative process. To do this, we used full-thickness osteochondral defects in a rat model and analyzed the effect of MFAT on cartilage repair.

Materials and Methods

Cell Cultures

All procedures were conducted according to the Ethics Committee of the 2nd Affiliated Hospital, Zhejiang University School of Medicine, Hangzhou, China. Knee and hip chondrocyte material was obtained from 6-week-old Sprague Dawley rats. Briefly, articular cartilage was cut into 1-mm³ particles. Then, the cartilage particles were digested and shaken with 0.2% collagenase II (Sigma-Aldrich, St. Louis, MO, USA) for 4 h at 37°C after 0.25% trypsin (Gibco RRL, Grand Island, NY, USA) treatment for 30 min. The chondrocytes were seeded into a culture flask and cultured in Dulbecco's Modified Eagle's Medium (DMEM)

supplemented with 10% FBS, 100U/mL penicillin, and 100U/mL streptomycin at 37°C in a humidified atmosphere with 5% CO₂. The medium was changed every 3 days.

Harvesting and Processing of the Adipose Tissue

After anesthesia with 4% pentobarbital sodium (Sigma-Aldrich), the abdomen of 9-week-old Sprague Dawley rats was sterilized and dissected for the adipose tissue. The harvested adipose tissue was transferred into Lipogems device and then processed as shown (Fig. 1). First, the closed system was filled with saline to eliminate air and the adipose tissue was pushed from the syringe into the device to obtain the first cluster reduction. When the desired amount of fat tissue was placed in the device, the whole bottle was fiercely shaken up and down for several minutes, and then the bottle was kept vertical until the floating fat was on the top of the device. With the switch on, the running saline took the generated oil and the blood residues away. The fat cluster was washed for another 3–5 times until the solution inside appeared clear. The second cluster reduction was obtained by pushing the floating fat cluster into a 10 mL syringe through the smaller reduction filter. The entire procedure, carried out in the closed, disposable and full-immersion device, progressively and gently reduced the diameter of the adipose tissue clusters from 1–3.5 mm to 0.2–0.8 mm.

Isolation and Culture of MFAT-Derived ASCs

According to the manufacturer's instructions³⁰, the MFAT was cultured in a culture flask containing DMEM supplemented with 10% FBS, 100 U/mL penicillin, 100 U/mL streptomycin, and 1% L-glutamine, and maintained in a humidified incubator at 37°C with 5% CO₂. The nonadherent fraction of the MFAT was discarded only after 2 weeks to ensure the ASCs could slip out. The medium was replaced every 4 days. When the culture reached confluence, cells were detached using trypsin-EDTA (Sigma-Aldrich) and sub-cultured for subsequent experiments.

Flow Cytometry Analysis

In order to determine ASCs phenotypes, about 1×10^6 ASCs derived from MFAT were detached, re-suspended and incubated at 4°C in the dark for 30 min with the following antibodies: Phycoerythrin (PE)-labeled anti-CD29, anti-CD31, anti-CD34, anti-CD45, and anti-CD90 (BD Bioscience, San Diego, CA, USA) and PE-labeled anti-CD44 (eBioscience, San Diego, CA, USA). Matched isotype IgG was used for control. Cell fluorescence was determined by FACScan flow cytometer (Becton-Dickinson, Franklin Lakes, NJ, USA).

Multilineage Differentiation

To determine the ability of differentiation to adipocytes, ASCs were seeded in a 6-well plate at the density of 4×10^4 with

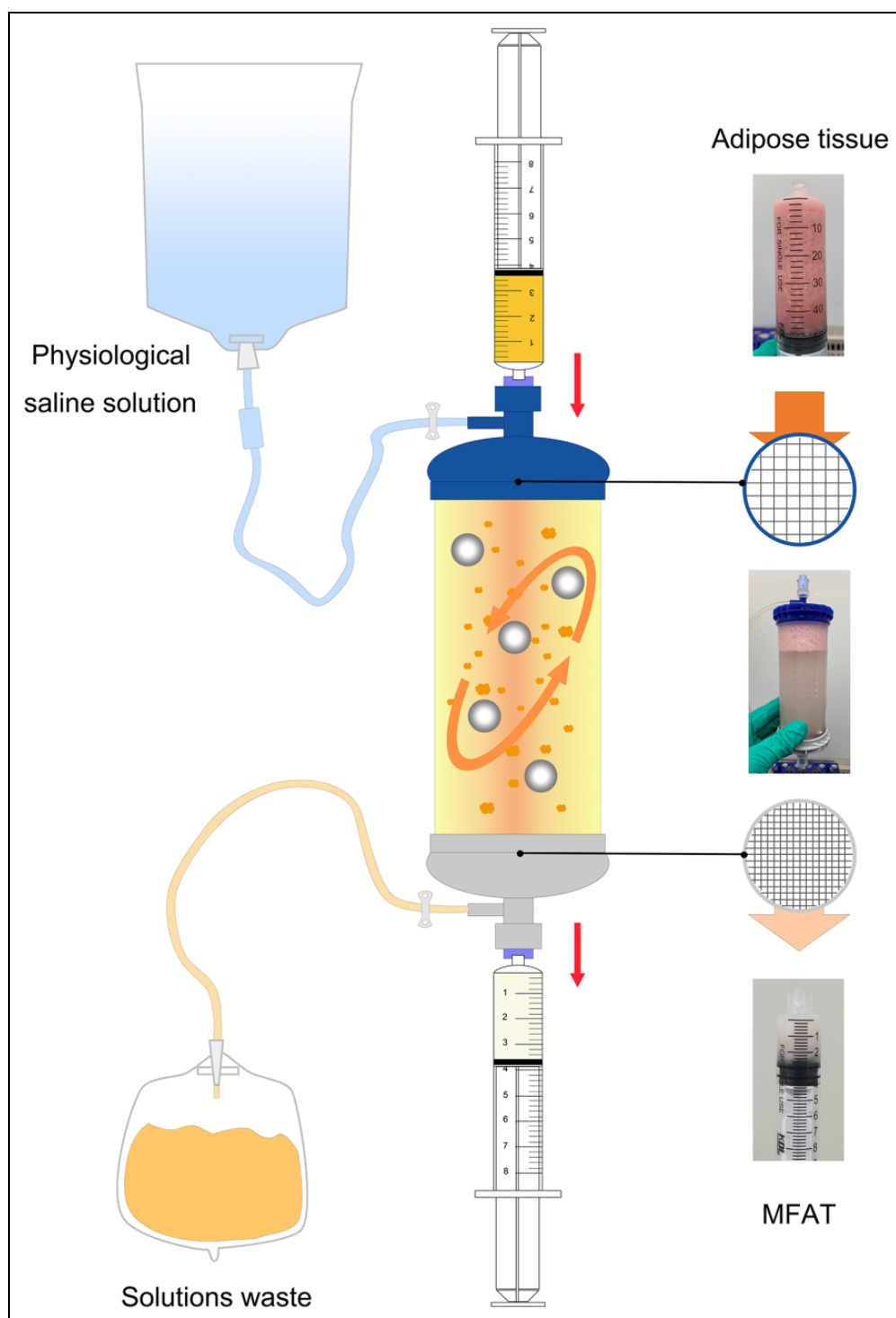


Figure 1. Schematic illustration of the Lipogems system for obtaining micro-fragmented adipose tissue (MFAT). First, the original adipose tissue was pushed through the blue filter for first cluster reduction. Then, the core device was fiercely shaken several times until the residual blood and oil were washed off by the running saline. The second cluster reduction was performed to obtain MFAT by pushing the inner adipose clusters into a syringe.

an adipogenic induction medium A (Cyagen, Chicago, IL, USA). Three days later, the medium was replaced by a maintenance medium B (Cyagen) for 24 h. After at least three times of repeated medium change, the cells were

fixed in 4% paraformaldehyde and stained by fresh Oil Red O solution.

To determine the ability of differentiation to osteoblasts, ASCs were seeded in a 6-well plate at the density of 4×10^4

with an osteogenic induction complete medium (Cyagen), replacing the medium every 3 days. After 3 weeks incubation, the cells were fixed in 4% paraformaldehyde and stained by Alizarin red solution.

To determine the ability of differentiation to chondrocytes, about 5×10^5 ASCs were pelleted in polypropylene conical tubes with a chondrogenic induction medium containing dexamethasone, ITS, transforming growth factor- β 3, proline ascorbate, sodium pyruvate, and l-glutamine (Sigma-Aldrich). The medium was replaced every 3–4 days for 3 weeks. Then the pellets were fixed in 4% paraformaldehyde solution and cut into 5 μ m sections for Alcian staining (Sigma-Aldrich).

Cell Scratch Assay

Chondrocytes were plated in 6-well plates (2×10^5 cells/well) and a scratch was made by using a 10 μ L sterile pipette until the confluence reached 90% at 37°C with 5% CO₂. Following washing with PBS for three times to remove the debris, the serum-free medium was added to the plate. Then, the MFAT (240 μ L/well) was added to the upper chamber of 6-well transwell system (8 μ m pore size, Costar, Kennebunk, ME, USA) in case of the direct contact with chondrocytes (PBS as control). After 24 h, the area of the scratch was photographed and measured by ImageJ (NIH, Bethesda, MD, USA) software.

Transwell Migration Assay

The MFAT (60 μ L/chamber) was added with 10% FBS medium into the upper chamber of 24-well transwell system (8 μ m pore size, Costar) and 10% FBS medium was also placed in the lower chamber. After 24 h of incubation, the upper chamber was removed and the medium in the lower chamber with secreted factors from MFAT was collected. Then, chondrocytes were seeded with serum-free medium into the upper chamber of another transwell at the density of 2×10^4 and the collected medium with secreted factors was added into the lower chamber. The cells were fixed with 4% paraformaldehyde and stained by 0.5% crystal violet (Sigma-Aldrich) after incubation at 37°C in 5% CO₂ for 12 h; cells that did not migrate through the pores were gently removed by a cotton swab. Migrated chondrocytes were visualized using a light microscope and analyzed by ImageJ software. Three repeated experiments were performed.

Animal Experiments

Twenty-six 8-week-old Sprague Dawley rats were used for the experiment. Twenty-four rats were anesthetized by pentobarbital and the femoral groove was exposed through a parapatellar skin incision after the patella was dislocated laterally. Then an osteochondral defect (1.5 mm diameter and 1 mm depth) was created in the center of the groove using a special drill. After the joint capsule and the skin

Table 1. International Cartilage Repair Society (ICRS) Macroscopic Evaluation for Osteochondral Defect Regeneration.

Criteria	Points
I. Degree of defect repair	
Level with surrounding cartilage	4
75% repair of defect depth	3
50% repair of defect depth	2
25% repair of defect depth	1
0% repair of defect depth	0
II. Integration to border zone	
Complete integration with surrounding cartilage	4
Demarcating border <1 mm	3
3/4 of graft integrated, 1/4 with a notable border >1 mm width	2
1/2 of graft integrated with surrounding cartilage, 1/2 with a notable border >1 mm	1
From no contact to 1/4 of graft integrated with surrounding cartilage	0
III. Macroscopic appearance	
Intact smooth surface	4
Fibrillated surface	3
Small, scattered fissures or cracks	2
Several, small or few but large fissures	1
Total degeneration of grafted area	0
IV. Overall score	
Grade I: normal	12
Grade II: nearly normal	11-8
Grade III: abnormal	7-4
Grade IV: severely abnormal	3-1

wound were closed, 50 μ L MFAT was immediately injected into the intra-articular space of one side joint and the contralateral joint was treated with 50 μ L PBS as control. The animals were randomly divided into four groups: defects treated with MFAT for 6 weeks ($n = 12$), defects treated with PBS for 6 weeks ($n = 12$), defects treated with MFAT for 12 weeks ($n = 12$), and defects treated with PBS for 12 weeks ($n = 12$). Another two unoperated rats were used as the normal group at 6 and 12 weeks. All animals were housed in cages with free movement.

Macroscopic and Histological Assessment

Animals were euthanized by pentobarbital at 6 and 12 weeks, the femur was harvested and fixed with 4% paraformaldehyde solution overnight, and the International Cartilage Repair Society (ICRS) macroscopic assessment (Table 1) was graded by three independent researchers for blind macroscopic evaluation. Following decalcification with 10% Ethylene Diamine Tetraacetic Acid (Sigma-Aldrich) for 2 months, the samples were cut into 5- μ m-thick sections. These sections were stained with hematoxylin/eosin (HE), safranin O/fast green (Saf-O) and a monoclonal antibody for type I, II, and VI collagen (Abcam, Cambridge, Mass, MA, USA). The cartilage repair was blindly scored by three independent researchers based on the modified O'Driscoll histologic scoring system (Table 2).

Table 2. The Modified O’Driscoll Histologic Score for Histologic Assessment for Cartilage Repair.

Characteristic	Score
I. Hyaline cartilage (%)	
80–100	8
60–80	6
40–60	4
20–40	2
0–20	0
II. Structural characteristics	
A. Surface irregularity	
Smooth and intact	2
Fissures	1
Severe disruption, fibrillation	0
B. Structural integrity	
Normal	2
Slight disruption, including cysts	1
Severe lack of integration	0
C. Thickness	
100% of normal adjacent cartilage	2
50% to 100% or thicker than normal	1
0–50%	0
D. Bonding to adjacent cartilage	
Bonded at both ends of graft	2
Bonded at one end/partially both ends	1
Not bonded	0
III. Freedom from cellular changes of degeneration	
Normal cellularity, no clusters	2
Slight hypocellularity, <25% chondrocyte clusters	1
Moderate hypocellularity, >25% clusters	0
IV. Freedom from degenerate changes in adjacent cartilage	
Normal cellularity, no clusters, normal staining	3
Normal cellularity, mild clusters, moderate staining	2
Mild or mod hypocellularity, slight staining	1
Severe hypocellularity, slight staining	0
V. Reconstitution of subchondral bone	
Complete reconstitution	2
Greater than 50% recon	1
50% or less recon	0
VI. Bonding of repair cartilage to de novo subchondral bone	
Complete and uninterrupted	2
<100% but >50% recon	1
<50% complete	0
VII. Safranin O staining	
>80% homogeneous positive stain	2
40%–80% homogeneous positive stain	1
<40% homogeneous positive stain	0
Total score	Max27

Statistical Analysis

All quantitative data were presented as means ± SDs. One-way ANOVA and post hoc Tukey’s test was used and the value of *p* < 0.05 was considered statistically significant.

Results

Characterization of MFAT-Derived ASCs

The ASCs that emerged from MFAT were cultured for 7–21 days and representative cells were observed and photographed with light microscopy. The morphology of these cells exhibited a typical spindle shape (Fig. 2A). To determine whether these ASCs could differentiate into adipocytes, osteoblasts, and chondrocytes, different incubation environments were used to induce them. Three types of positive staining experiments, Red O, Alizarin Red S, and Alcian staining, proved the multipotential differentiation capability (Fig. 2B–D). Flow cytometry analysis showed that MFAT-derived ASCs were positive for the expression of MSC markers CD29, CD44, and CD90, but negative for the hematopoietic markers CD31, CD34, and CD45 (Fig. 2E).

The Effect of MFAT on Migration of Chondrocytes In Vitro

Using a wound-healing assay, we determined the effect of MFAT on the migratory ability of the chondrocytes. Compared with the control group, the MFAT group significantly increased cell migration into the wound area after 24 h in chondrocytes (*p* < 0.01, Fig. 3A, B). In the transwell chamber analysis, MFAT enhanced the ability of chondrocytes to migrate with respect to that in the control group after 12 h (49.56 ± 2.882 vs. 99 ± 1.347 cells per field; *p* < 0.001, Fig. 3C, D).

The Effect of MFAT on Repair of Cartilage Defects in the Rat Model

To determine the ability of MFAT to repair full-thickness cartilage defects in vivo, rat defects treated with MFAT or PBS were harvested at 6 and 12 weeks for analysis.

At 6 weeks after treatment, the macroscopic appearance of the repaired tissue demonstrated that the defects were filled by neotissue to different degrees. The surface of the defects in MFAT group was more intact and smoother than in the control group (Fig. 4A). However, the ICRS assessment score was 8.611 ± 0.2982 in the MFAT group and 7.861 ± 0.2766 in the control group, with no significant difference (*p* = 0.0787, Fig. 4B). HE, safranin O, and immunohistochemical staining were employed for the histological evaluation. Compared with the normal cartilage, the MFAT-treated defects showed good subchondral bone reconstruction and hyaline cartilage formation with low expression of type I collagen and high expression of type II collagen. Most chondrocytes were observed to have a regular distribution and morphology accompanied by pericellular matrix staining of type VI collagen. In contrast, subchondral bone had hardly grown into the defect region and hyaline cartilage had rarely formed in the control group. The defect region was mostly filled by fibrotic tissue with higher expression of type I collagen and lower expression of type II collagen (Fig. 4C).

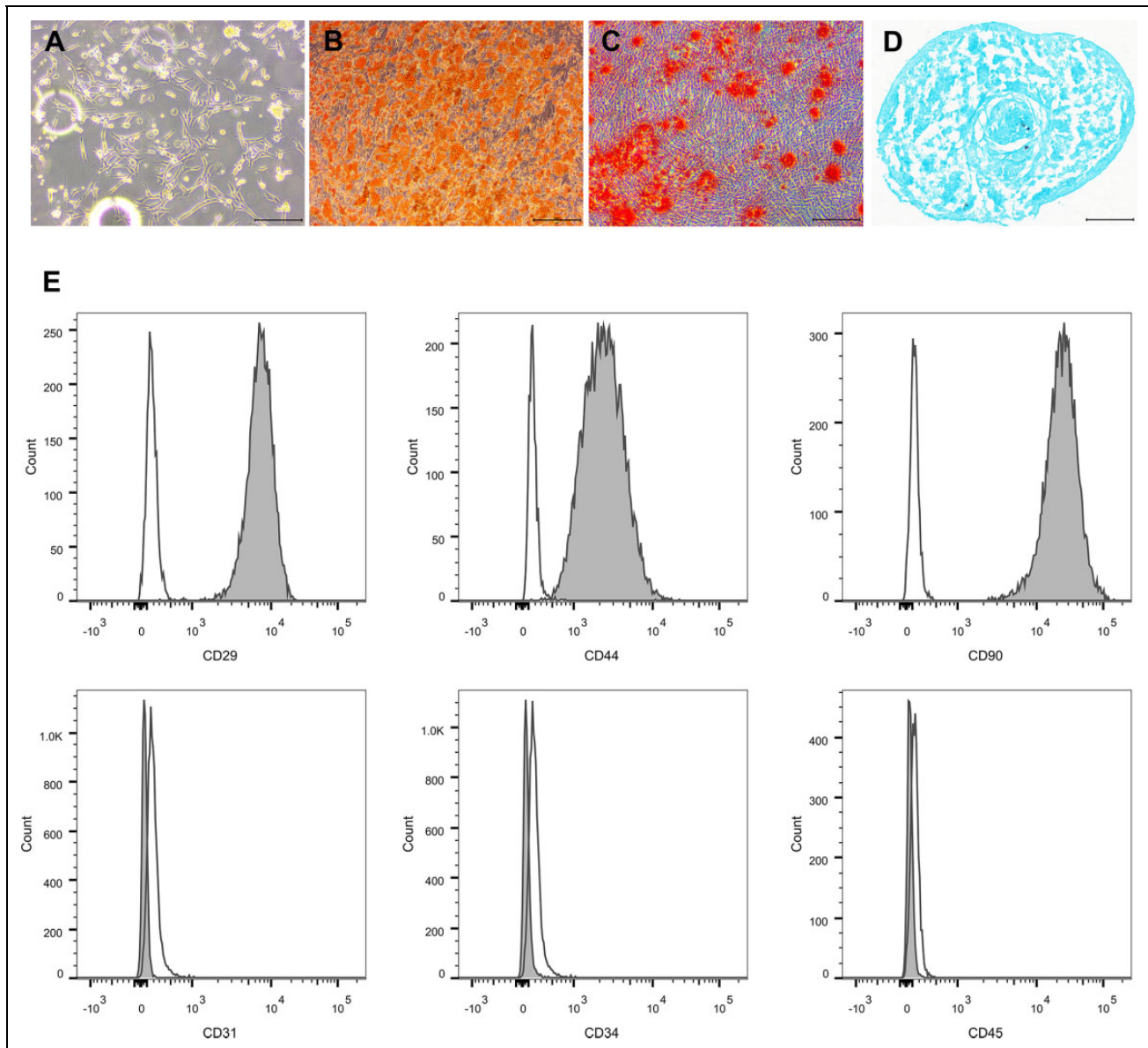


Figure 2. Characterization and identification of adipose-derived stem cells (ASCs) from MFAT. (A) Representative photograph of primary ASCs exhibited a typical spindle shape morphology ($\times 40$). (B, C) After the adipogenic and osteogenic induction, the lipid droplets and calcium nodules secreted from differentiated ASCs were visible with Oil Red O and Alizarin red staining, respectively ($\times 40$). (D) The differentiated chondrogenic pellets were cut into $5 \mu\text{m}$ sections and stained positive with Alcian blue staining. (E) The surface makers of ASCs were detected by flow cytometry analysis and the result demonstrated positive expression of CD29, CD44, and CD90, but negative expression of CD31, CD34, and CD45.

The modified O'Driscoll score of the MFAT group and the control group was 15.42 ± 1.547 and 8.194 ± 1.217 , respectively (Fig. 4D). There was a significant difference in effect of repair between two groups ($p < 0.01$).

At 12 weeks post-surgery, macroscopic observation showed nearly normal smooth cartilage surface and complete integration with surrounding cartilage in the MFAT group, and irregular surface and white neotissue filling in the control group (Fig. 5A). The ICRS assessment score of that MFAT group was significantly higher than the control

group (10.14 ± 0.2943 vs. 8.806 ± 0.3793 , $p < 0.05$, Fig. 5B). Histological evaluation showed the great degree of cartilage defect repair in MFAT group: there was complete subchondral bone reconstruction, a high amount of hyaline cartilage, a low level of type I collagen, and a high level of type II collagen. The chondrocytes were observed to have a regular distribution and morphology accompanied by pericellular matrix staining of type VI collagen. On the contrary, the PBS-treated defects showed incomplete subchondral bone reconstruction, lower amount of hyaline cartilage,

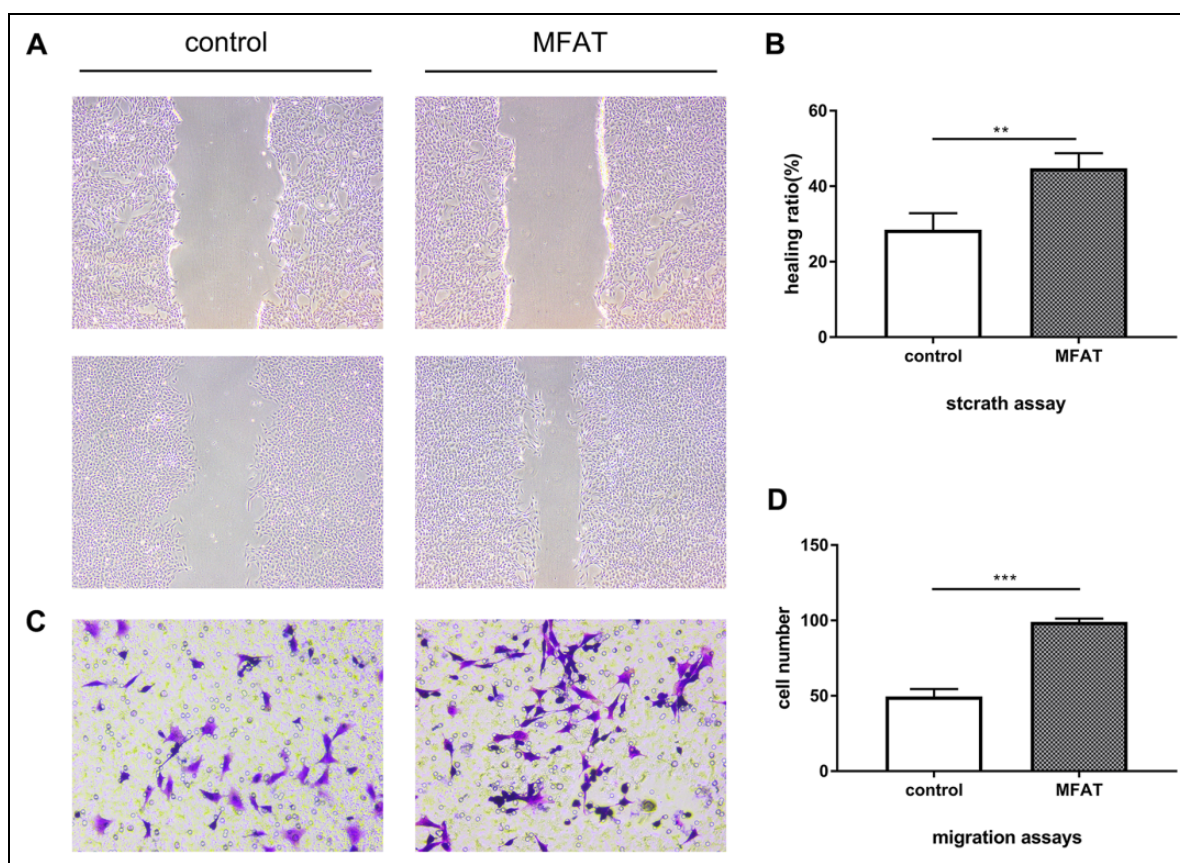


Figure 3. Effects of MFAT on chondrocytes migration and progression. (A) Representative pictures of scratch assays. Chondrocytes migrated into the scratch area with treatment of MFAT or PBS for 24 h after scratched at confluence. (B) The healing ratio in the MFAT group was significantly higher than the control group (** $p < 0.01$). (C) In transwell assays, migrated cells were visible with crystal violet staining; representative pictures are shown. (D) The cell number of migration in the MFAT group was significantly higher than the control group (** $p < 0.001$).

higher level of type I collagen and lower level of type II collagen, which indicated a worse effect of cartilage repair (Fig. 5C). The modified O'Driscoll score of the MFAT group was significantly higher than the control group (15.42 ± 1.169 vs. 11.61 ± 1.186 , $p < 0.05$, Fig. 5D).

Discussion

Our study suggests for the first time that the intra-articular injection of MFAT promotes repair of full-thickness osteochondral defects in a rat model.

Osteoarthritis, a chronic degeneration of articular cartilage, is a leading cause of severe disability and social burden^{31,32}. During the osteoarthritis process, the integrity of cartilage is destroyed followed by cartilage composition change, involving the constituent of extracellular matrix (ECM) rich in proteoglycans and collagens, which is associated with disordered catabolic activity and inflammation in the joint^{33,34}. As we know, in mammalian articular cartilage, the number of dividing chondrocytes may be less than 1% of the population, which explain its limited capacity for

intrinsic healing and repair combined with the avascular and aneural nature of cartilage^{35,36}. Current therapeutic strategies for cartilage damage have limitations and deficiencies including mismatched architectural features, insufficient mechanical properties, and inadequate biological functions³⁷.

To address these limitations, the therapeutic application of MSCs is a rapidly increasing area of investigation; many studies have displayed evidence of the benefit of MSCs in cartilage repair due to their self-renewal properties, multilineage differentiation potential, and immunomodulatory capacity³⁸⁻⁴¹. MSCs were originally identified in bone marrow, and exist in many other tissues such as adipose, umbilical cord, placenta, periosteum, and tendon^{42,43}. The points of most concern in stem cell-based therapies are how to enrich the suitable cell source, increase the differentiation ratio, and reduce side effects of tissue harvest. These conditions make adipose tissue the most desirable source of stem cells. ASCs are usually localized in the stromal vascular fraction of subcutaneous adipose tissue and are separated out through enzymatic digestion⁴⁴. Generally, isolated ASCs

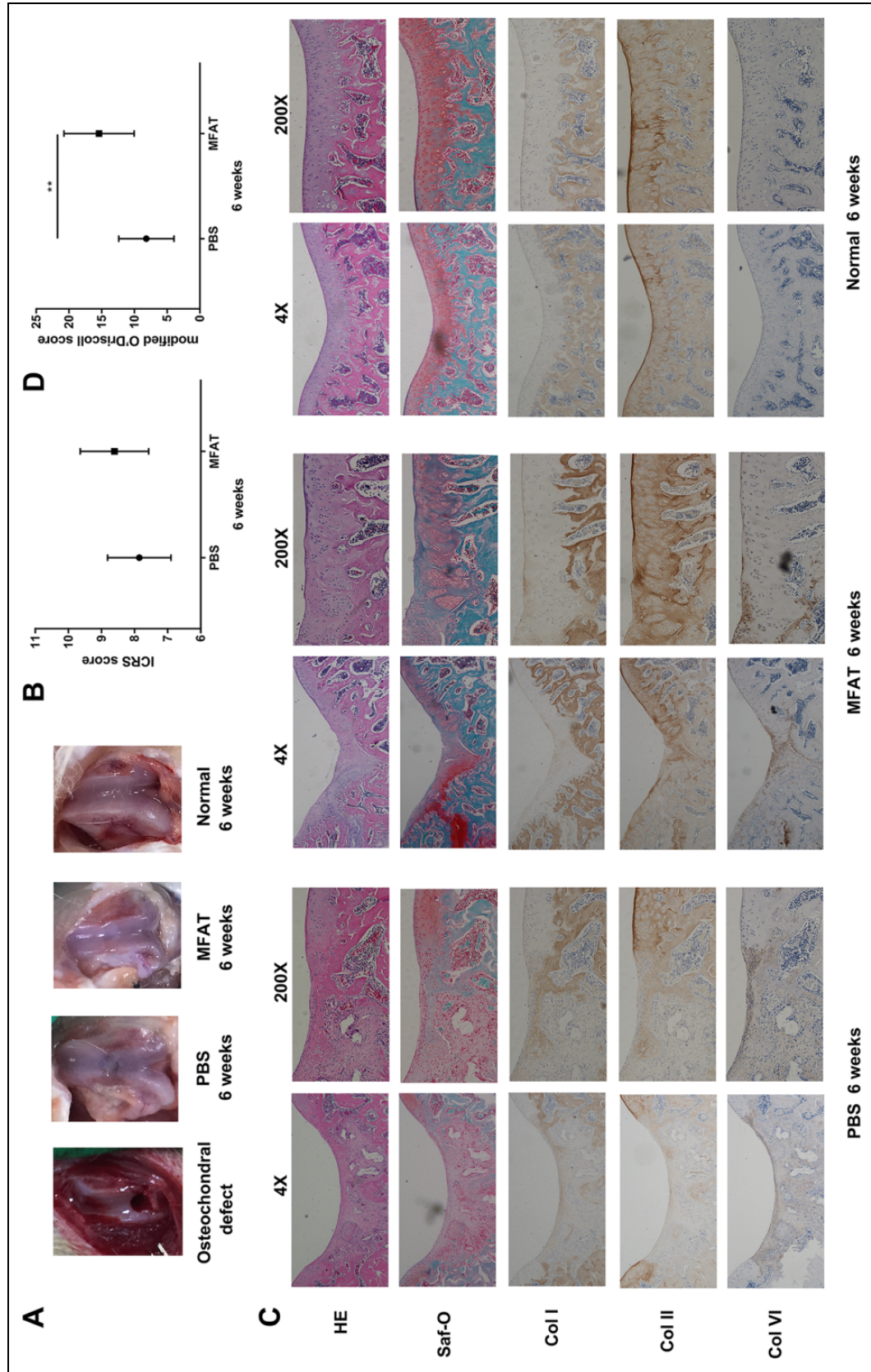


Figure 4. Effect of MFAT on osteochondral defects repair in vivo at 6 weeks post-surgery. (A) Macroscopic appearance of femoral condyle cartilage. (B) ICRS macroscopic assessment scores in cartilage samples. There was no significance between two groups ($n = 12$, $p = 0.0787$). (C) HE, Safranin O, and immunohistochemical staining of repaired cartilage. (D) Modified O'Driscoll histologic scores in cartilage samples. The result showed that MFAT group had a significantly higher average score compared with the control group ($n = 12$, $**p < 0.01$). Values represent means \pm standard deviation.

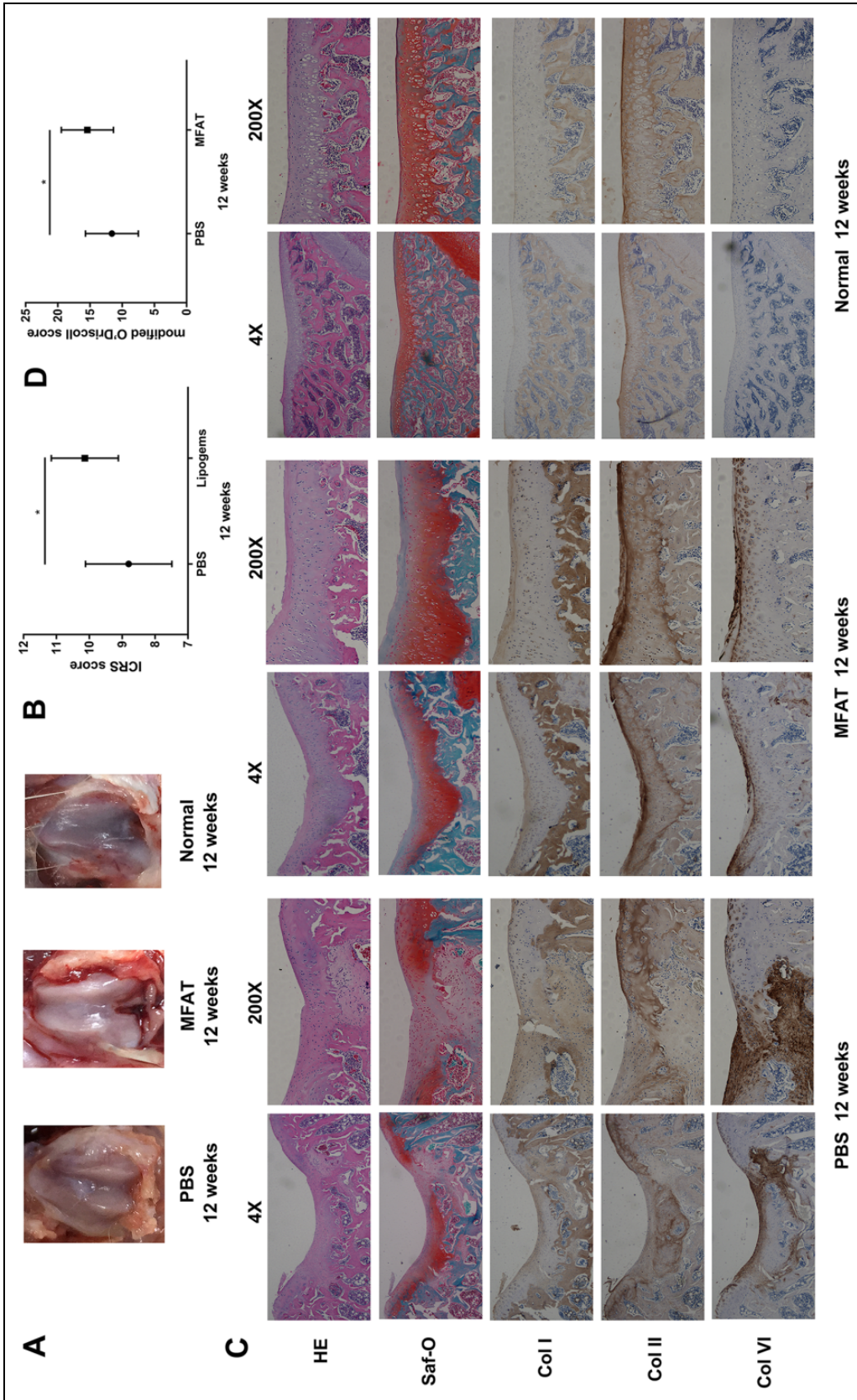


Figure 5. Effect of MFAT on osteochondral defects repair in vivo at 12 weeks post-surgery. (A) Macroscopic appearance of femoral condyle cartilage. (B) ICRS macroscopic assessment scores in cartilage samples. Average score of MFAT group was significantly higher than the control group ($n = 12$, $*p < 0.05$). (C) HE, Safranin O, and immunohistochemical staining of repaired cartilage. (D) Modified O'Driscoll histologic scores in cartilage samples. The result showed that MFAT group had a significantly higher average score compared with the control group ($n = 12$, $*p < 0.05$). Values represent means \pm standard deviation.

are combined with various biomaterial scaffolds to enhance their regenerative efficacy in osteochondral defects in the injured area, to address the problems of short-lived survival and limited differentiation capacity when using stem cells alone. However, there is no optimal stimulation of ASCs to differentiate into chondrocytes prior to implantation, with complicated processing steps (enzymatic digestion, cell expansion, and differentiation), which increases the translational barriers⁴⁵.

Differently from scaffold-based ASCs treatment, the entire processing of MFAT is completed in a closed, full-immersion, and physical environment, without enzymes or other additives. The MFAT exhibited a notably preserved vascular stromal niche, retaining elements with pericyte perivascular identity comprising high percentages of MSCs³⁰. Shah et al. demonstrated MFAT as a direct source of ASCs through characterizing the surface marker and multilineage differentiation of ASCs from human lipoaspirates⁴⁶. Here, we determined the same result in rat. It may therefore be hypothesized that these inherent ASCs will repopulate the lesion of cartilage to differentiate into chondrocytes following intra-articular injection of MFAT. The self-renewal and differentiation of stem cells are basically controlled by the niche through both intrinsic factors and the surrounding microenvironment^{47,48}. Furthermore, the vascular stromal niche provides sophisticated signals to manipulate the ratio of proliferation and multidirectional differentiation potentials, refraining from the aging and death during expansion in vitro. The MFAT acts as a slow-released “natural scaffold,” and continuously delivers growth factors, extracellular vesicles, and much other modulatory information into the microenvironment surrounding damaged cartilage when injected into the injured joint. Our migration experiment suggested that MFAT could recruit chondrocytes to the defect region from adjacent normal cartilage without direct intercellular contact. Likewise, Randelli et al. found that the proliferation of progenitor cells was significantly increased without change of multipotency when co-cultured with MFAT released factors⁴⁹, and Ceserani et al. have shown their capacity to induce vascular stabilization and to inhibit inflammation through a paracrine activity⁵⁰. These results show that the natural scaffold in osteochondral defect treatment using MFAT is as important as the ASCs. Despite the promising possibilities, however, there are no studies that evaluate the effect of MFAT on full-thickness osteochondral defects in vivo, which are needed before this approach may be deemed safe and effective for clinical use.

To study the effect objectively, we observed that MFAT injection in vivo significantly increases expression of hyaline cartilage, type II, and VI collagen in the defect area; this has been shown to play a leading role in the regenerative process, being the major ECM of normal cartilage. The time period of 12 weeks was selected based on a previous study, in which the osteochondral defect cartilage was sufficiently fully repaired in a rat model after 12 weeks⁵¹. In our study,

enhanced macroscopic and histological evaluations (e.g., intact smooth surface, complete reconstitution of subchondral bone, and suitable collagen expression) showed the repaired cartilage could fit its biological function at 12 weeks after intra-articular MFAT injection. Nevertheless, future studies would need to dissect the components present in MFAT and investigate their underlying mechanisms in cartilage repair.

In conclusion, we isolated and characterized the ASCs derived from MFAT, determined enhanced migration on chondrocytes, and confirmed the promoted effect on osteochondral defect repair, which suggests a ready-to-use and effective therapy for cartilage repair to satisfy current needs.

Ethical Approval

All of the procedures and protocols for this study were approved by the Ethics Committee of the 2nd Affiliated Hospital, Zhejiang University School of Medicine, Hangzhou, China.

Statement of Human and Animal Rights

All animal procedures in this study were conducted according to the approved protocols by the Ethics Committee of the 2nd Affiliated Hospital, Zhejiang University School of Medicine.

Statement of Informed Consent

There are no human subjects in this article and informed consent is not applicable.

Declaration of Conflicting Interests

The author(s) declared no potential conflicts of interest with respect to the research, authorship, and/or publication of this article.

Funding

The author(s) disclosed receipt of the following financial support for the research, authorship, and/or publication of this article: This study was supported by the National Natural Science Foundation of China (No. 81772340).

ORCID iD

Xuesong Dai  <https://orcid.org/0000-0003-1404-0049>

References

1. Hunter DJ, Bierma-Zeinstra S. Osteoarthritis. *Lancet*. 2019; 393(10182):1745–1759.
2. Guermazi A, Hayashi D, Roemer FW, Niu J, Quinn EK, Crema MD, Nevitt MC, Torner J, Lewis CE, Felson DT. Brief report: partial- and full-thickness focal cartilage defects contribute equally to development of new cartilage damage in knee osteoarthritis: the multicenter osteoarthritis study. *Arthritis Rheumatol*. 2017;69(3):560–564.
3. Gomoll AH, Minas T. The quality of healing: articular cartilage. *Wound Repair Regen*. 2014;22(suppl 1):30–38.
4. Armiento AR, Alini M, Stoddart MJ. Articular fibrocartilage - Why does hyaline cartilage fail to repair? *Adv Drug Deliv Rev*. 2018.

5. Jones IA, Togashi R, Wilson ML, Heckmann N, Vangsness CT Jr. Intra-articular treatment options for knee osteoarthritis. *Nat Rev Rheumatol*. 2019;15(2):77–90.
6. Quilliot J, Couderc M, Giraud C, Soubrier M, Mathieu S. Efficacy of intra-articular hyaluronic acid injection in knee osteoarthritis in everyday life. *Semin Arthritis Rheum*. 2019;49(1):e10–e11.
7. Sundman EA, Cole BJ, Karas V, Della Valle C, Tetreault MW, Mohammed HO, Fortier LA. The anti-inflammatory and matrix restorative mechanisms of platelet-rich plasma in osteoarthritis. *Am J Sports Med*. 2014;42(1):35–41.
8. Ludin A, Sela JJ, Schroeder A, Samuni Y, Nitzan DW, Amir G. Injection of vascular endothelial growth factor into knee joints induces osteoarthritis in mice. *Osteoarthritis Cartilage*. 2013;21(3):491–497.
9. Ruta DJ, Villarreal AD, Richardson DR. Orthopedic surgical options for joint cartilage repair and restoration. *Phys Med Rehabil Clin N Am*. 2016;27(4):1019–1042.
10. Schinhan M, Gruber M, Dorotka R, Pilz M, Stelzener D, Chiari C, Rossler N, Windhager R, Nehrer S. Matrix-associated autologous chondrocyte transplantation in a compartmentalized early stage of osteoarthritis. *Osteoarthritis Cartilage*. 2013;21(1):217–225.
11. Gudas R, Gudaite A, Mickevicius T, Masiulis N, Simonaityte R, Cekanauskas E, Skurvydas A. Comparison of osteochondral autologous transplantation, microfracture, or debridement techniques in articular cartilage lesions associated with anterior cruciate ligament injury: a prospective study with a 3-year follow-up. *Arthroscopy*. 2013;29(1):89–97.
12. Huang BJ, Hu JC, Athanasiou KA. Cell-based tissue engineering strategies used in the clinical repair of articular cartilage. *Biomaterials*. 2016;98:1–22.
13. Simon TM, Jackson DW. Articular cartilage: injury pathways and treatment options. *Sports Med Arthrosc Rev*. 2018;26(1):31–39.
14. Lee WY, Wang B. Cartilage repair by mesenchymal stem cells: clinical trial update and perspectives. *J Orthop Translat*. 2017;9:76–88.
15. Toh WS, Foldager CB, Pei M, Hui JH. Advances in mesenchymal stem cell-based strategies for cartilage repair and regeneration. *Stem Cell Rev*. 2014;10(5):686–696.
16. Estes BT, Diekmann BO, Gimble JM, Guilak F. Isolation of adipose-derived stem cells and their induction to a chondrogenic phenotype. *Nat Protoc*. 2010;5(7):1294–1311.
17. Brady K, Dickinson SC, Guillot PV, Polak J, Blom AW, Kafienah W, Hollander AP. Human fetal and adult bone marrow-derived mesenchymal stem cells use different signaling pathways for the initiation of chondrogenesis. *Stem Cells Dev*. 2014;23(5):541–554.
18. Roberts SJ, van Gestel N, Carmeliet G, Luyten FP. Uncovering the periosteum for skeletal regeneration: the stem cell that lies beneath. *Bone*. 2015;70:10–18.
19. Lee JC, Min HJ, Park HJ, Lee S, Seong SC, Lee MC. Synovial membrane-derived mesenchymal stem cells supported by platelet-rich plasma can repair osteochondral defects in a rabbit model. *Arthroscopy*. 2013;29(6):1034–1046.
20. Orbay H, Devi K, Williams PA, Dehghani T, Silva EA, Sahar DE. Comparison of endothelial differentiation capacities of human and rat adipose-derived stem cells. *Plast Reconstr Surg*. 2016;138(6):1231–1241.
21. Mellor LF, Mohiti-Asli M, Williams J, Kannan A, Dent MR, Guilak F, Lobo EG. Extracellular calcium modulates chondrogenic and osteogenic differentiation of human adipose-derived stem cells: a novel approach for osteochondral tissue engineering using a single stem cell source. *Tissue Eng Part A*. 2015;21(17–18):2323–2333.
22. Xu LJ, Wang SF, Wang DQ, Ma LJ, Chen Z, Chen QQ, Wang J, Yan L. Adipose-derived stromal cells resemble bone marrow stromal cells in hepatocyte differentiation potential in vitro and in vivo. *World J Gastroenterol*. 2017;23(38):6973–6982.
23. Bortolotti F, Ukovich L, Razban V, Martinelli V, Ruozi G, Pelos B, Dore F, Giacca M, Zaccagna S. In vivo therapeutic potential of mesenchymal stromal cells depends on the source and the isolation procedure. *Stem Cell Reports*. 2015;4(3):332–339.
24. Arcidiacono JA, Blair JW, Benton KA. US Food and Drug Administration international collaborations for cellular therapy product regulation. *Stem Cell Res Ther*. 2012;3(5):38.
25. Sensebe L, Bourin P, Tarte K. Good manufacturing practices production of mesenchymal stem/stromal cells. *Hum Gene Ther*. 2011;22(1):19–26.
26. Riis S, Zachar V, Boucher S, Vemuri MC, Pennisi CP, Fink T. Critical steps in the isolation and expansion of adipose-derived stem cells for translational therapy. *Expert Rev Mol Med*. 2015;17:e11.
27. Tremolada C, Colombo V, Ventura C. Adipose tissue and mesenchymal stem cells: state of the art and lipogems(R) technology development. *Curr Stem Cell Rep*. 2016;2:304–312.
28. Tremolada C, Ricordi C, Caplan AI, Ventura C. Mesenchymal stem cells in lipogems, a reverse story: from clinical practice to basic science. *Methods Mol Biol*. 2016;1416:109–122.
29. Kaewsuwan S, Song SY, Kim JH, Sung JH. Mimicking the functional niche of adipose-derived stem cells for regenerative medicine. *Expert Opin Biol Ther*. 2012;12(12):1575–1588.
30. Bianchi F, Maioli M, Leonardi E, Olivi E, Pasquinelli G, Valente S, Mendez AJ, Ricordi C, Raffaini M, Tremolada C, Ventura C. A new nonenzymatic method and device to obtain a fat tissue derivative highly enriched in pericyte-like elements by mild mechanical forces from human lipoaspirates. *Cell Transplant*. 2013;22(11):2063–2077.
31. Hunter DJ, Schofield D, Callander E. The individual and socioeconomic impact of osteoarthritis. *Nat Rev Rheumatol*. 2014;10(7):437–441.
32. Prieto-Alhambra D, Judge A, Javaid MK, Cooper C, Diez-Perez A, Arden NK. Incidence and risk factors for clinically diagnosed knee, hip and hand osteoarthritis: influences of age, gender and osteoarthritis affecting other joints. *Ann Rheum Dis*. 2014;73(9):1659–1664.
33. Guilak F, Nims RJ, Dicks A, Wu CL, Meulenbelt I. Osteoarthritis as a disease of the cartilage pericellular matrix. *Matrix Biol*. 2018;71–72:40–50.

34. Rahmati M, Nalesso G, Mobasheri A, Mozafari M. Aging and osteoarthritis: central role of the extracellular matrix. *Ageing Res Rev.* 2017;40:20–30.
35. Farquharson C. Bones and cartilage: developmental and evolutionary skeletal biology, Second Edition by Brian K. Hall. *Br Poult Sci.* 2015;56(6):151001221650007.
36. Oldershaw RA. Cell sources for the regeneration of articular cartilage: the past, the horizon and the future. *Int J Exp Pathol.* 2012;93(6):389–400.
37. Yang J, Zhang YS, Yue K, Khademhosseini A. Cell-laden hydrogels for osteochondral and cartilage tissue engineering. *Acta Biomater.* 2017;57:1–25.
38. Zhang K, Zhang Y, Yan S, Gong L, Wang J, Chen X, Cui L, Yin J. Repair of an articular cartilage defect using adipose-derived stem cells loaded on a polyelectrolyte complex scaffold based on poly(l-glutamic acid) and chitosan. *Acta Biomater.* 2013;9(7):7276–7288.
39. Cui L, Wu Y, Cen L, Zhou H, Yin S, Liu G, Liu W, Cao Y. Repair of articular cartilage defect in non-weight bearing areas using adipose derived stem cells loaded polyglycolic acid mesh. *Biomaterials.* 2009;30(14):2683–2693.
40. Du WJ, Reppel L, Leger L, Schenowitz C, Huselstein C, Bensoussan D, Carosella ED, Han ZC, Rouas-Freiss N. Mesenchymal stem cells derived from human bone marrow and adipose tissue maintain their immunosuppressive properties after chondrogenic differentiation: role of HLA-G. *Stem Cells Dev.* 2016;25(19):1454–1469.
41. Pastides P, Chimutengwende-Gordon M, Maffulli N, Khan W. Stem cell therapy for human cartilage defects: a systematic review. *Osteoarthritis Cartilage.* 2013;21(5):646–654.
42. Chen FH, Tuan RS. Mesenchymal stem cells in arthritic diseases. *Arthritis Res Ther.* 2008;10(5):223.
43. Macrin D, Joseph JP, Pillai AA, Devi A. Eminent sources of adult mesenchymal stem cells and their therapeutic imminecence. *Stem Cell Rev Rep.* 2017;13(6):741–756.
44. Dicker A, Le Blanc K, Astrom G, van Harmelen V, Gotherstrom C, Blomqvist L, Arner P, Ryden M. Functional studies of mesenchymal stem cells derived from adult human adipose tissue. *Exp Cell Res.* 2005;308(2):283–290.
45. Bosetti M, Borrone A, Follenzi A, Messaggio F, Tremolada C, Cannas M. Human lipoaspirate as autologous injectable active scaffold for one-step repair of cartilage defects. *Cell Transplant.* 2016;25(6):1043–1056.
46. Shah F, Wu X, Dietrich M, Rood J, Gimble J. A non-enzymatic method for isolating human adipose tissue-derived stromal stem cells. *Cytotherapy.* 2013;15(8):979–985.
47. Naveiras O, Daley GQ. Stem cells and their niche: a matter of fate. *Cell Mol Life Sci.* 2006;63(7–8):760–766.
48. Spradling A, Drummond-Barbosa D, Kai T. Stem cells find their niche. *Nature.* 2001;414(6859):98–104.
49. Randelli P, Menon A, Ragone V, Creo P, Bergante S, Randelli F, De Girolamo L, Alfieri Montrasio U, Banfi G, Cabitza P, Tettamanti G, et al. Lipogems product treatment increases the proliferation rate of human tendon stem cells without affecting their stemness and differentiation capability. *Stem Cells Int.* 2016;2016:4373410.
50. Ceserani V, Ferri A, Berenzi A, Benetti A, Ciusani E, Pascucci L, Bazzucchi C, Cocce V, Bonomi A, Pessina A, Ghezzi E, et al. Angiogenic and anti-inflammatory properties of micro-fragmented fat tissue and its derived mesenchymal stromal cells. *Vasc Cell.* 2016;8:3.
51. Toh WS, Lee EH, Guo XM, Chan JK, Yeow CH, Choo AB, Cao T. Cartilage repair using hyaluronan hydrogel-encapsulated human embryonic stem cell-derived chondrogenic cells. *Biomaterials.* 2010;31(27):6968–6980.